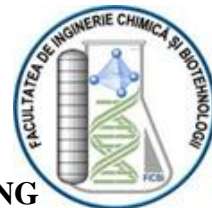




NATIONAL UNIVERSITY OF SCIENCE AND TECHNOLOGY

POLYTEHNICA BUCHAREST

DOCTORAL SCHOOL OF THE FACULTY OF CHEMICAL ENGINEERING
AND BIOTECHNOLOGY



**VALORIFICATION OF CHITOSAN FROM MARINE
SOURCES FOR OBTAINING NEW AGENTS IN
WASTEWATER TREATMENT**

-Summary-

Coordinator:

Prof. Dr. Ing. Horia IOVU

PhD student:

Chim. Marinela Victoria DUMITRU

President	Prof. Dr. Ing. Cristian Pîrvu	from	UNST POLITEHNICA Bucharest
Scientific coordinator	Prof. Dr. Ing. Horia Iovu	from	UNST POLITEHNICA Bucharest
Referent	Prof. Dr. Ing. Sorina Gârea	from	UNST POLITEHNICA Bucharest
Referent	CS I Dr. Ing. Andrei Sârbu	from	INCDCP-ICECHIM- Bucharest
Referent	CS I Dr. Ing. Tanța-Verona Iordache	from	INCDCP-ICECHIM- Bucharest

Bucharest,

2024

THESIS CONTENT IN EXTENSO

THESIS CONTENT IN EXTENSO.....	2
ABBREVIATIONS.....	3
1. INTRODUCTION.....	4
ORIGINAL CONTRIBUTIONS.....	5
4. MOLECULARLY IMPRINTED PSEUDO-CRYOGELS BASED ON NATURAL POLYMERS FOR SELECTIVE RETENTION OF PENICILLIN G	7
5. HYBRID CRYOSTRUCTURES WITH SUPERABSORBENT PROPERTIES AS PROMISING MATERIALS FOR PENICILLIN RETENTION G	13
6. RETENTION OF CIPROFLOXACIN AND CARBAMAZEPINE FROM AQUEOUS SOLUTIONS USING CHITOSAN-BASED CRYOSTRUCTURED COMPOSITES	22
REFERENCES	30

ABBREVIATIONS

APTES- 3-aminopropiltriethoxisilan

BC – Biocellulose

CC –Commercial Chitosan

CBZ – Carbamazepine

CCH – Chitosan prepared in the laboratory from commercial chitin

CH₃-COOH –acetic acid

CIP – Ciprofloxacin

CSH – Chitosan from shrimp shells waste enriched with calcium carbonate

FQ – fluoroquinolone

K-uscat – Kaolin

K-MAPTS – Kaolin modified with silane 3-trimethoxysilylpropyl methacrylate

MB – Methylene blue

MIP – Molecular imprinted pseudo-cryogels

MMT – Montmorillonite

M-CSbMs – Chitosan-based magnetic materials

NH₄HCO₃ – Ammonium bicarbonate

NIP – Non-molecularly imprinted pseudo-cryogels

OS – Organosilicate prepared by sol-gel method

PG – Penicillin G

TC – Tetracycline

TEOS – Tetraethylorthosilicate

1. INTRODUCTION

Natural polymers have attracted worldwide attention because of the outstanding properties they possess. One of the most important properties of these polymers is biodegradability.

The preparation of materials based on natural polymers and silicates such as composite cryostructures has become a trend as these materials can be used for a variety of applications. In this PhD thesis the aim was to prepare new cryostructured materials for the retention of drugs from wastewater because as is known water pollution has become quite a big problem in recent years. Dyes, heavy metals or drugs, all these pollutants are a very big concern.

To this end, this PhD thesis focused on the preparation of new materials based on natural polymers and silicates in order to retain drugs such as: ciprofloxacin, carbamazepine and penicillin G.

Historically, water pollution is caused by humans due to industrialisation.

Nowadays, there are many methods used to treat polluted water, such as: electrochemical method, polymer membrane separation and adsorption. Electrochemical methods require fewer chemicals and do not cause secondary pollution, but are expensive and technically difficult. Compared to the methods mentioned above, the adsorption process has been widely used due to its high pollutant removal efficiency and flexible operation.

The following report presents the results obtained from the three studies carried out.

Note that the numbering of the headings, figures and tables corresponds to the work in extenso

Keywords: composite cryostructures, chitosan, ciprofloxacin, carbamazepine, penicillin G, water purification

ORIGINAL CONTRIBUTIONS

THE AIM AND OBJECTIVES OF THE THESIS

In the present context, the thesis entitled **Valorification of chitosan from marine sources for obtaining new agents in wastewater treatment** had as its **main goal** the synthesis and characterization of new materials based on natural polymers and silicates for drug retention for water purification, following **three main research objectives**:

O1. Preparation and characterization of molecularly imprinted pseudo-cryogels based on natural polymers for selective retention of penicillin G from aqueous solutions.

O2. Synthesis and evaluation of hybrid cryostructures with superabsorbent properties as promising materials for the retention of penicillin G from aqueous solutions.

O3. Improved synthesis method and evaluation of silicate and chitosan based composite cryostructures for retention of ciprofloxacin and carbamazepine from aqueous solutions.

Thus, the first main objective of this thesis focused on obtaining molecularly imprinted pseudo cryogels based on natural polymers for selective PG retention. To this end, using the molecular imprinting technique, molecularly imprinted cryostructures with PG were obtained. Polymer matrix based on chitosan and biocellulose was used to carry out the study due to their low toxicity and availability in nature.

Two types of chitosan were used in this study, namely commercial chitosan and chitosan obtained in the laboratory from commercial chitin. Natural polymers were dissolved in weakly acidic solution, over which biocellulose, specific amount of PG (only in MIP samples) and the pore-forming agent (ammonium bicarbonate) were added. Samples were frozen, cut and freeze-dried. To obtain cavities with specific PG recognition in the final material, the template molecule was extracted by repeated washes with water. Using characterization techniques (FTIR, TGA, UV-Vis, re-binding tests) the pseudo-cryogels confirmed, specific chemical composition, thermal stability and high retention capacities of PG from aqueous solutions.

The originality highlighted in this objective refers to the synthesis method, which involved the preparation by molecular imprinting technique of new spongy cryostructures based on natural polymers with applications in specific retention of PG from aqueous solutions.

The second main objective of the thesis involved the preparation of supermacroporous cryostructures and their evaluation for PG retention. Compared to the previous study, in this case the cryostructures (NIP) were compounded with a modified natural silicate to improve their stability in water. The same polymer mixture was used for this purpose. The silicate used was kaolin, which was functionalized with a organophilization agent (MAPTS) to ensure compatibility with the biopolymer matrix.

Valorificarea chitosanului din surse marine pentru obținerea unor noi agenți de tratare a apelor

In this study, in addition to the two types of chitosan used previously, namely commercial chitosan and chitosan obtained in the laboratory from commercial chitin, a type of chitosan also obtained in the laboratory from shrimp shells waste enriched with calcium carbonate was tested. Preparation of the cryostructures involved dissolving the chitosan in acidic solution, with biocellulose added only in some samples, followed by modified clay (K-MAPTS) in various amounts. After homogenization of the solutions, the pore-forming agent was added. Finally the samples were frozen, cut and freeze-dried. The characterization techniques allowed the determination of the chemical composition of the materials (FTIR), thermal properties (TGA), morphology (SEM), porosity (BET) and last but not least the adsorption mechanism for PG from aqueous solutions (UV-Vis and pseudo-order kinetic model II).

*The originality of **the second objective** consisted in obtaining new materials based on natural polymers (in particular based on chitosan obtained in the laboratory from shrimp shells waste) and modified natural silicates with improved physical properties for PG retention.*

***The third main objective** of the thesis involved the preparation of cryostructures for the retention of carbamazepine and ciprofloxacin. To obtain these cryostructures, chitosan, functionalized kaolin similar as in the second objective and a synthetic silicate obtained by the sol-gel technique from tetraethyldithiothiosilicate (TEOS) and 3-aminopropyltriethoxysilane (APTES) were used. In this objective, an improvement of the mechanical properties of the cryostructures was achieved by replacing the functionalized kaolin with synthetic silicate particles. In this chapter the cryostructures were prepared in a similar way as in the previous objective, except that biocellulose was no longer used, only two types of chitosan were used (commercial chitosan and chitosan obtained from shrimps shells waste enriched with calcium carbonate) and another synthetic silicate was tested as a reinforcing agent (OS).*

The chemical composition and morphology of the materials were determined by characterization techniques (FTIR, SEM). Mechanical tests demonstrate improved mechanical properties of the cryostructures and kinetic models confirmed the CIP and CBZ retention mechanism.

*The originality of **this objective** consisted in replacing the modified clay with another synthetic silicate in order to improve the mechanical properties of the cryostructures. The cryostructures obtained were also tested for the retention of other types of drugs.*

4. MOLECULARLY IMPRINTED PSEUDO-CRYOGELS BASED ON NATURAL POLYMERS FOR SELECTIVE RETENTION OF PENICILLIN G

The first part of this PhD thesis contains the synthesis and characterization of new molecularly imprinted pseudo-cryogels based on biopolymers (chitosan and biocellulose) capable of acting as selective recognition materials for the retention of penicillin G from aqueous solutions.

Four series of molecularly imprinted (MIP1÷MIP4) and non-imprinted (NIP1÷NIP4) pseudo-cryogels were prepared as shown in **Figure 4.1**.

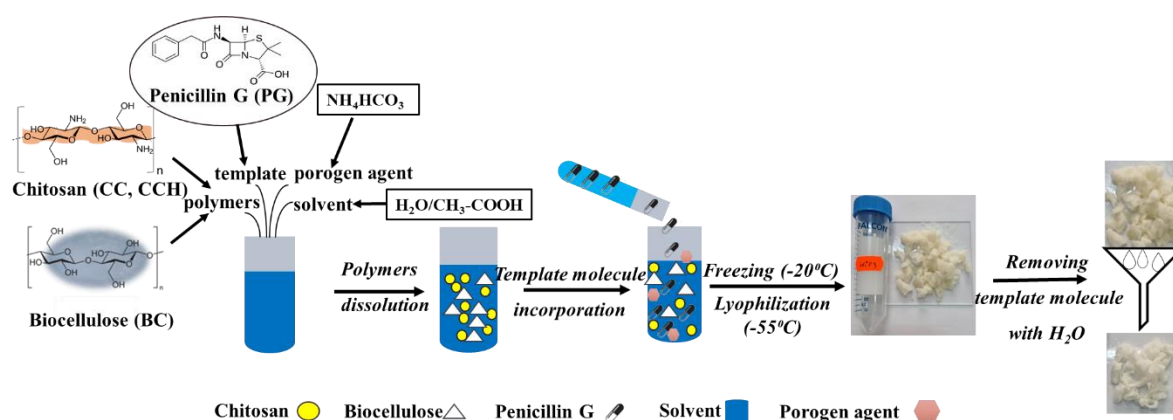


Figure 4.1. Synthesis of molecularly imprinted and non-imprinted pseudo-cryogels

The characterization of imprinted and non-imprinted molecular pseudo-cryogels was performed using FTIR spectroscopy, thermogravimetric analysis, determination of swelling degrees, re-binding experiments and kinetics.

FTIR Spectroscopy

FTIR analysis of the pseudo-cryogels obtained allowed structural evaluation as well as the existence of possible interactions occurring between the components of the system. The FTIR spectra of the MIP and NIP pseudo-cryogels before and after being washed can be seen in **Figure 4.2**. (A), (B), (C) and (D). For comparison, the FTIR spectra of the MIP pseudo-cryogels containing PG, the MIP extract (washed after 5 h) and the FTIR spectrum of Penicillin G, used as reference, are shown.

The FTIR spectra for NIP and MIP samples in **Figure 4.2** (A,B,C,D) show the characteristic bands of chitosan and biocellulose. The presence of penicillin G can be seen in the case of the MIP pseudo-cryogels, which means that the imprinting process was successfully achieved.

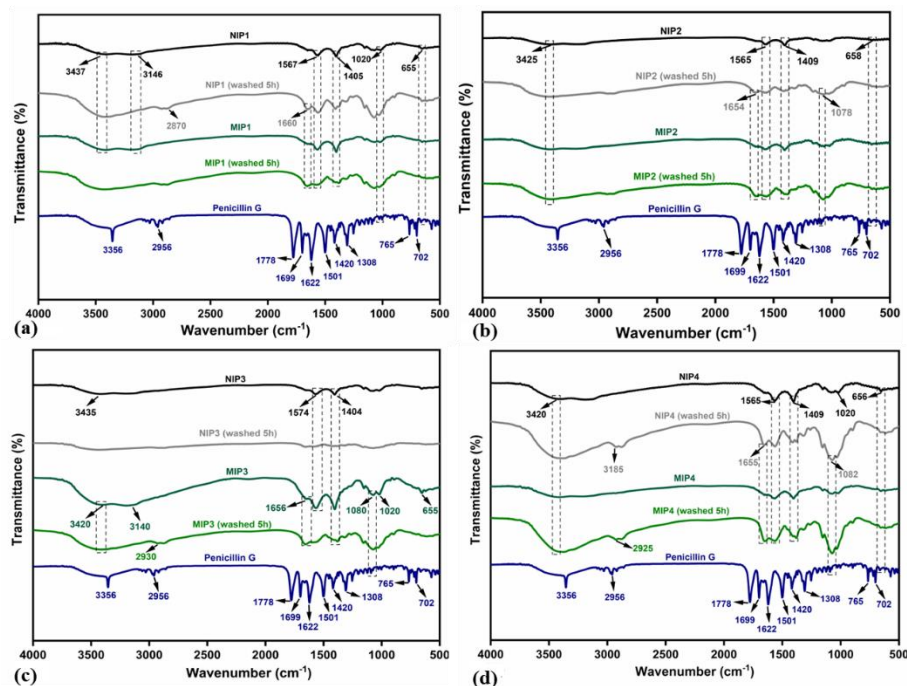


Figure 4.2. FTIR spectra for MIP1/NIP1(a), MIP2/NIP2 (b), MIP3/NIP3 (c), MIP4/NIP4 (d) before and after being washed, compared with PG.

Thermogravimetric Analysis (TGA/DTG)

The effect of the template molecule and also of the two biopolymers on the stability of the pseudo-cryogels was investigated by thermogravimetric analysis. As can be seen in **Figure 4.3. (a, b, c, d)** and **Table 4.3.** the maximum degradation temperatures for MIP1÷MIP4 imprinted samples is lower than for non-imprinted NIP1÷NIP4, this behavior may be due to the degradation of the PG template molecule [207]. The thermal stability of imprinted and non-imprinted pseudo-cryogels highlighted the effect of imprinting on the studied materials as a complementary method for FTIR analysis.

Table 4.3. Thermal degradation of molecularly imprinted (MIP) and non-imprinted pseudo cryogels (NIP)

Sample	T _{1Max} °C	T _{2Max} °C	F%
NIP1	151	279	71,92
MIP1	134	248	71,60
NIP2	153	276	71,40
MIP2	142	246	80,50
NIP3	191	282	87,40
MIP3	114	247	76,80
NIP4	124	275	74,00
MIP4	124	243	77,20

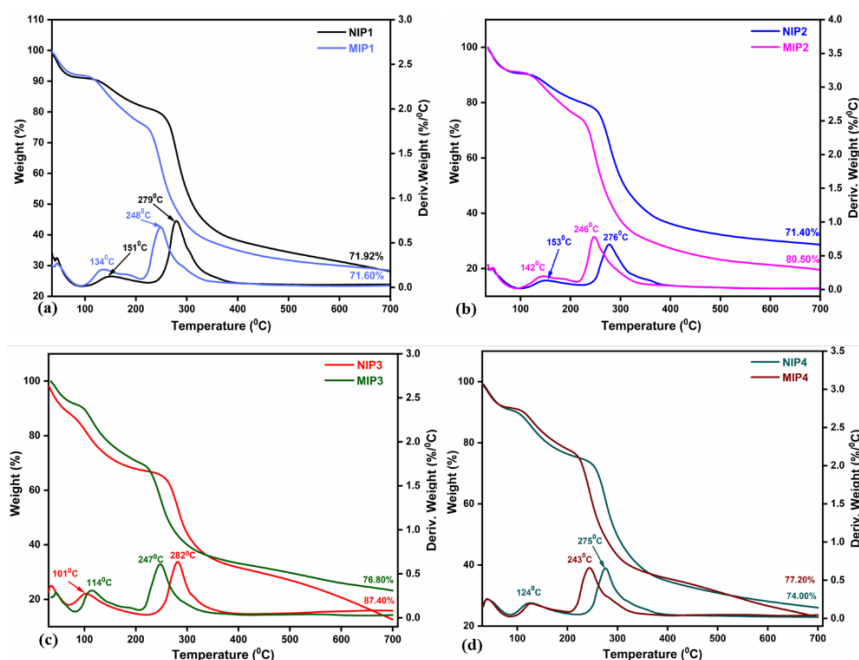


Figure 4.3. TGA/DTG results for NIP1/ MIP1 (a), NIP2/ MIP2 (b), NIP3/ MIP3 (c) și NIP4/ MIP4 (d).

Swelling degrees study (SD)

Monitoring the swelling process over time and determining the time required for the pseudo-cryogels to be in contact with water was done because they disintegrate after only a few hours as they are not chemically cross-linked. The values of the swelling degrees for samples NIP1÷NIP4 and MIP1÷MIP4, can be seen in **Table 4.4**.

Table 4.4. Swelling degrees until 180 minutes for pseudo-cryogels MIP and NIP

Time (min)	SD (g H ₂ O/ g pseudo-cryogel)							
	NIP1	MIP1	NIP2	MIP2	NIP3	MIP3	NIP4	MIP4
5	6,91	7,17	7,65	6,82	4,20	4,21	6,92	5,21
15	9,48	9,59	11,92	9,91	5,50	5,44	8,39	6,89
30	17,61	13,39	17,80	14,01	5,89	7,58	12,82	9,95
60	30,78	18,03	15,23	14,27	8,20	12,11	20,10	15,35
120	39,62	21,10	28,14	14,35	8,42	17,61	25,02	19,78
180	39,88	23,36	28,92	-	9,01	20,18	27,29	20,62

As it may be seen in **Table 4.4**, both series of imprinted and non-imprinted pseudo-cryogels showed high swelling degrees but biocellulose does not improve the stability of pseudo-cryogels in water.

Re-binding and kinetics studies

MIP pseudo-cryogels were evaluated by performing re-binding experiments in the time interval 0-1440 minutes. The variation of the adsorption capacity (Q) with time and the values of the imprinting factors (IF) of the pseudo-cryogel materials (NIP and MIP) are shown in

Valorificarea chitosanului din surse marine pentru obținerea unor noi agenți de tratare a apelor

Figure 4.5. and **Table 4.5.** Both MIP and NIP samples showed an increased stability in water compared to GG, this behavior was due to the change of pH solution by PG from 5.5 (distilled water) to 6.5 (20 mmol/L PG solution) [244]. In terms of adsorption capacity (Q), the pseudo-cryogels prepared with biocellulose, namely MIP 2 and MIP 4, were able to adsorb a much higher amount of PG from the solution, about 67 mmol PG/g cryogel compared to the chitosan-based ones (MIP 1 and MIP 3) of about 40 mmol PG/g cryogel, which was found to be twice as high compared to other studies [244].

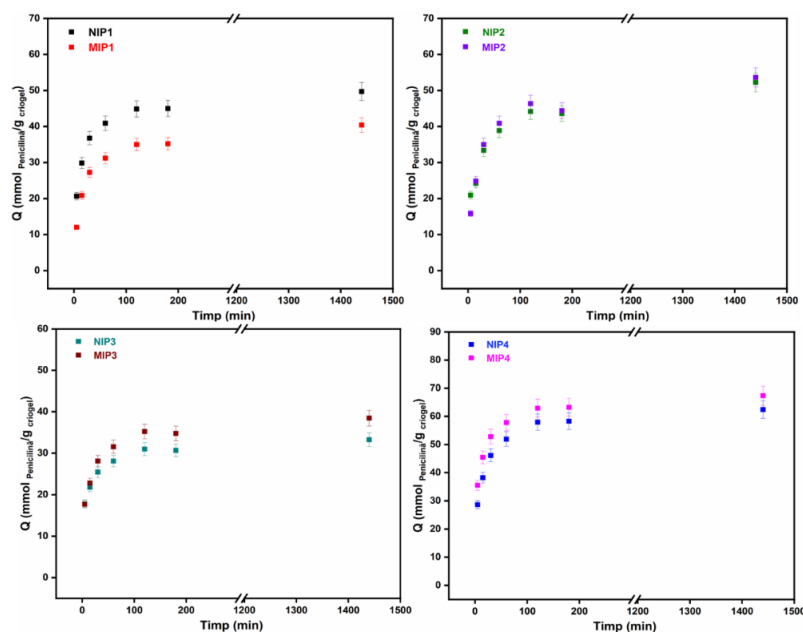


Figure 4.5. Variation of adsorption capacity for MIP/NIP samples in the time interval 0-1440 min using 5% (standard error)

Further, it can be considered that the chitosan-based molecular imprinted samples prepared in the laboratory were able to adsorb a higher amount of PG compared to NIP references. The highest imprinting factor (IF) values were recorded for samples MIP 3 and MIP 4, as can also be seen in **Table 4.5.**

Table 4.5. Specificity of re-binding assessed by IF calculation

Time (min)	IF			
	MIP1	MIP2	MIP3	MIP4
5	0,582	0,755	0,996	1,240
15	0,698	1,028	1,045	1,189
30	0,740	1,048	1,103	1,144
60	0,763	1,051	1,123	1,113
120	0,780	1,049	1,137	1,086
180	0,782	1,018	1,133	1,085
1440	0,813	1,026	1,125	1,079

Valorificarea chitosanului din surse marine pentru obținerea unor noi agenți de tratare a apelor

Next, the experimental values in **Figure 4.6.** were analysed using a pseudo-second order kinetic model, in which the adsorption capacity at 1440 min was used as the equilibrium adsorption capacity. **Equation (4)** [245] was used to calculate the adsorption kinetic parameters (summarized in **Table 4.6.**) for commercial chitosan-based samples (NIP1, MIP1, NIP2 and MIP2 - **Figure 4.6.**) and laboratory-prepared chitosan-based samples (NIP3, MIP3, NIP4 and MIP4- **Figure 4.7.**).

These results underline that the PG adsorption process, by all the pseudo-cryogel materials tested, follows a pseudo- second order kinetic model, with a linear $t/q(t)$ vs. t equation and high accuracy (all R^2 values are above 0.999).

Table 4.6. Parameters of the pseudo-second order kinetic model

Sample	k_2 (g mmol ⁻¹ min ⁻¹)	q_e (mmol/g)	R^2
NIP1	$1,62 \cdot 10^{-3}$	49,68	0,99993
MIP1	$1,39 \cdot 10^{-3}$	40,39	0,99989
NIP2	$0,94 \cdot 10^{-3}$	52,19	0,99968
MIP2	$0,91 \cdot 10^{-3}$	53,59	0,99970
NIP3	$3,10 \cdot 10^{-3}$	33,25	0,99995
MIP3	$2,16 \cdot 10^{-3}$	38,42	0,99992
NIP4	$1,53 \cdot 10^{-3}$	62,41	0,99997
MIP4	$1,72 \cdot 10^{-3}$	67,34	0,99997

*For this evaluation, the adsorption capacity at 24 hours was used as the equilibrium adsorption capacity.

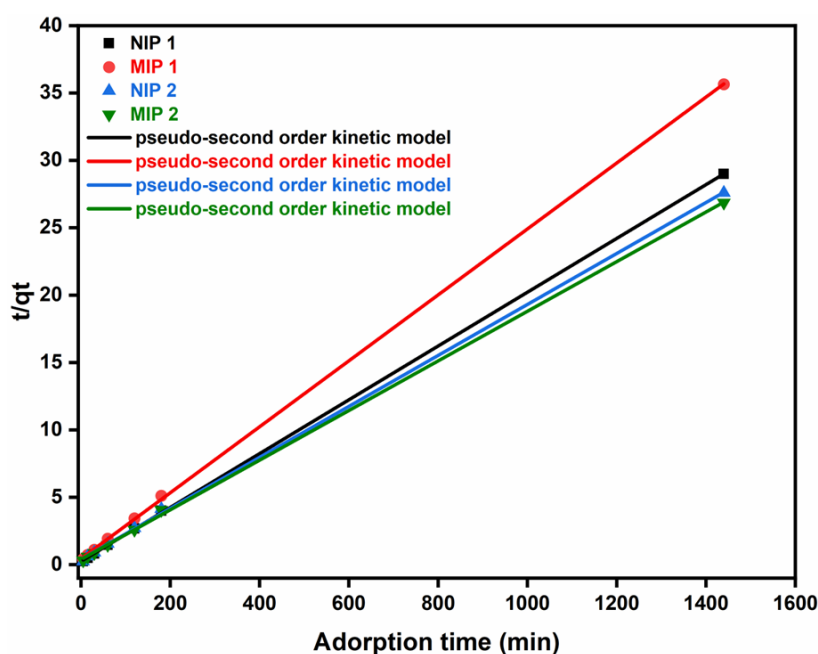


Figure 4.6. Pseudo second-order kinetic model of the adsorption process for NIP1/MIP1 and NIP2/ MIP2 samples

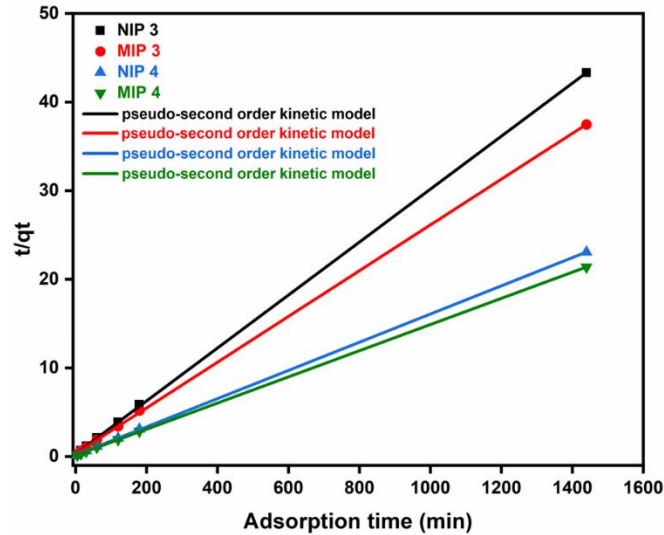


Figure 4.7. Pseudo-second order kinetic model of the adsorption process for NIP3/MIP3 and NIP4/MIP4 samples

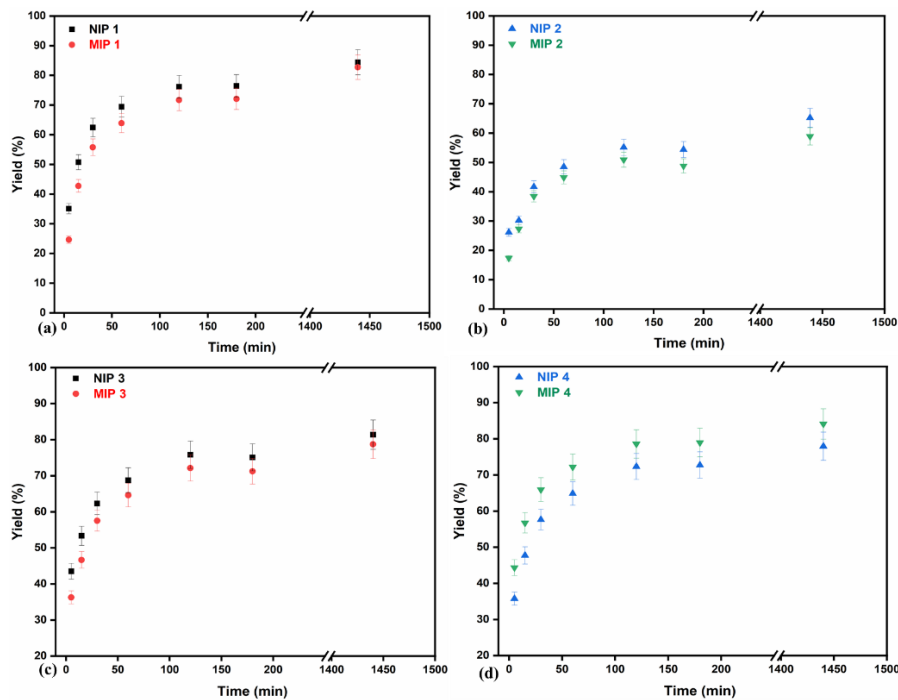


Figure 4.8. Yield of NIP1-MIP4 pseudo-cryogels using 5% (standard error).

The retention yield of the pseudo-cryogels can be seen in **Figure 4.8.**, where the highest retention value was observed for NIP1 (84.38%) and MIP1 (82.73%) samples. The non-imprinted CCH-based pseudo-cryogels containing biocellulose and those without biocellulose showed similar behaviours [NIP 3 (81.70%) and NIP 4 (77.93%)]. However, in the case of the molecularly imprinted pseudo-cryogels, a significantly higher retention capacity can be confirmed for the MIP 4 sample (84.01%) and a similar behaviour for MIP3 NIP 3 (78.70%). By this characterization it can be confirmed that the samples have high retention capacities on penicillin G, of about 90%.

5. HYBRID CRYOSTRUCTURES WITH SUPERABSORBENT PROPERTIES AS PROMISING MATERIALS FOR PENICILLIN G RETENTION

The second part of this PhD thesis contains the synthesis and characterization of hybrid cryostructures with superabsorbent properties as promising materials for penicillin G retention. Three series of cryostructures based on commercial chitosan (P1-K-BC÷P3-K), chitosan prepared from commercial chitin (P4-K-BC÷P6-K) and chitosan prepared from shrimps shells waste enriched with calcium carbonate (P7-K-BC÷P9-K) biocellulose and modified kaolin as shown in **Figure 5.1**. were prepared for PG retention.

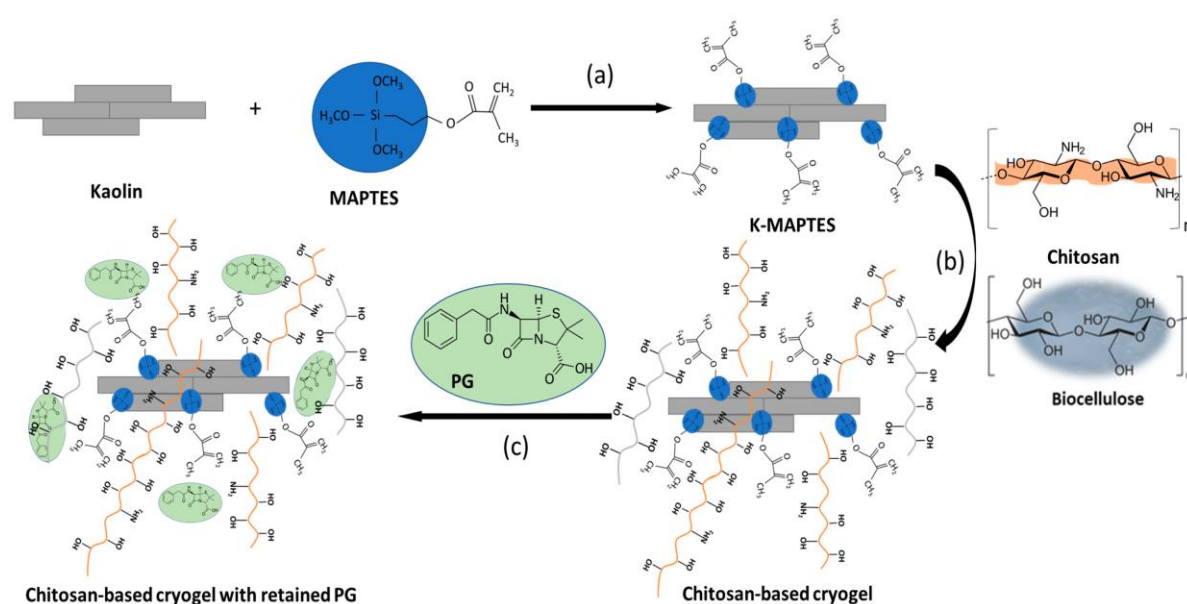


Figure 5.1. Silylation of kaolin using MAPTS (a); proposed mechanism of interaction of K-MAPTS with chitosan and biocellulose (b); proposed mechanism of PG retention using biopolymer-based cryostructures (c) [244].

FTIR spectroscopy

FTIR spectra of hybrid cryostructures prepared using different amounts of K and similar chitosan types can be seen in **Figure 5.2**. (**Figure 5.2a**-series of CC-based samples: **Figure 5.2b**-series of CCH-based samples, **Figure 5.2c**-series of CSH-based samples).

The appearance of the characteristic bands of the silylation agent confirms kaolin was successfully silylated, and the appearance of the characteristic bands of clay in the cryostructure spectra shows that it has been incorporated into polymer matrix.

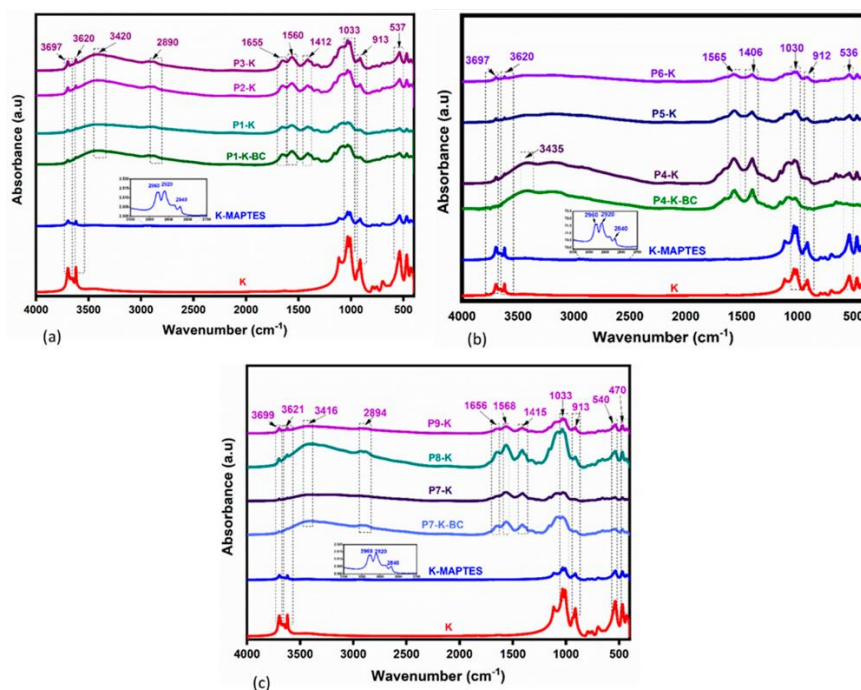


Figure 5.2. FTIR spectra of hybrid cryostructures (a) series P1-K-BC÷P3-K; series (b) P4-K-BC÷P6-K, și series (c) P7-K-BC÷P9-K compared with K and K-MAPTS.

Thermogravimetric Analysis (TGA/DTG)

TGA/DTG analysis was used to investigate the thermal behavior of hybrid cryostructures based on natural polymers and modified clay. The values for maximum decomposition temperatures and mass loss for the cryostructures and references K and K-MAPTS may be observed in **Figure 5.3.**, **Figure 5.4. a-d.** and **Table 5.3.**

Table 5.3. Maximum decomposition temperatures and mass losses in each decomposition step as evaluated from TG analysis, for the three cryogel series and of K and K-MAPTES

Sample	T _{1Max} °C	T _{2Max} °C	T _{3Max} °C	T ₁ %	T ₂ %	T ₃ %	F%
K	-	-	522,3	-	0,51	10,45	10,96
K-MAPTS	-	410,8	512,8	-	1,20	11,50	12,70
P1-K-BC	165,7	292,7	461,3	10,47	43,40	9,30	63,17
P1-K	161,8	292,5	466,8	13,64	41,63	9,35	64,62
P2-K	165,9	292,6	466,4	10,95	37,46	9,36	57,77
P3-K	158,4	295,5	486,4	9,47	34,42	9,47	53,36
P4-K-BC	101,7	284,3	479,2	35,36	32,68	8,18	76,22
P4-K	106,0	285,3	464,5	34,68	33,48	7,80	75,96
P5-K	100,8	288,7	496,2	33,73	29,25	7,20	70,18
P6-K	102,3	289,3	494,5	27,19	27,91	7,95	63,05
P7-K-BC	183,7	328,9	432,3	71,41	11,95	6,62	89,98
P7-K	192,4	332,2	434,8	62,96	14,71	13,55	91,22
P8-K	195,0	334,4	433,4	70,90	10,43	4,81	86,14
P9-K	204,4	335,8	442,4	63,49	12,36	4,96	80,81

Valorificarea chitosanului din surse marine pentru obținerea unor noi agenți de tratare a apelor

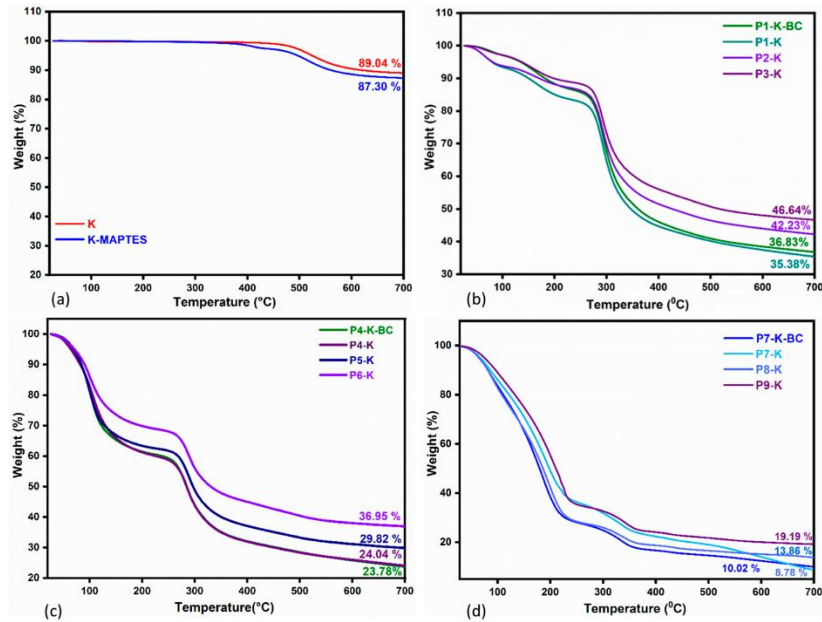


Figure 5.3. Thermal degradation of K and modified K-MAPTES (a) compared to the hybrid cryostructures (b) series P1-K-BC÷P3-K; (c) series P4-K-BC÷P6-K (d) series P7-K-BC÷P9-K.

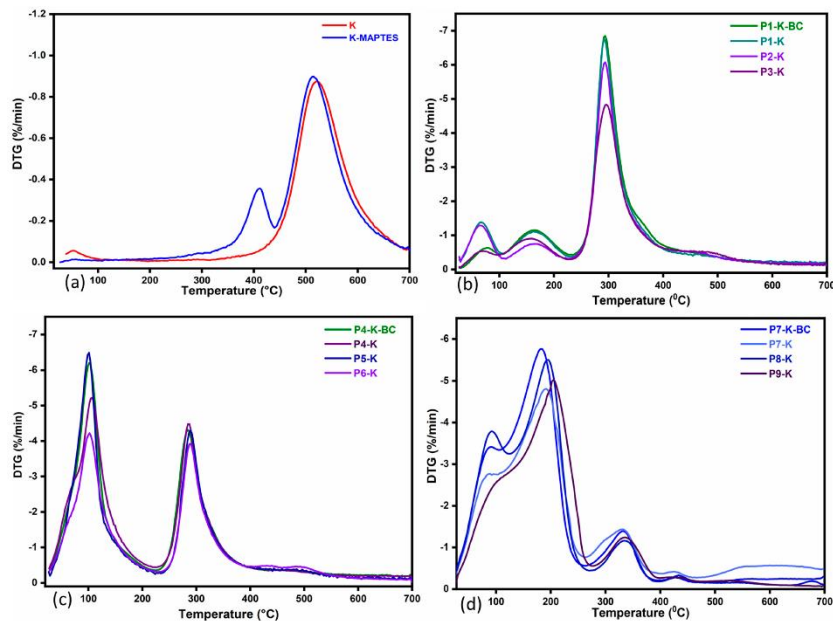


Figure 5.4. Derivative curves for K and modified K-MAPTES degradation (a) compared to the hybrid cryostructures degradation (b) series P1-K-BC÷P3-K; (c) series P4-K-BC÷ P6-K (d) series P7-K-BC÷P9-K.

Subsequently, a slight mass loss was observed for all cryostructures between 400-550 °C, indicating that the sample K-MAPTES decomposes according to the mechanism described above. Thus, the TGA/DTG results show that the incorporation of K-MAPTES into the chitosan polymer matrix was successfully achieved, which implicitly led to improved thermal stability of the hybrid cryostructures; the effect being more intense for the CSH-based (i.e. P9-K) samples.

Scanning Electron Microscopy (SEM)

În **Figure 5.5.**, the macroporous structures of cryostructures recorded by SEM can be observed for the series with CC (P1-K-BC÷P3-K), with CCH (P4-K-BC÷P6-K) and with CSH (P7-K-BC÷P9-K). The clay (K-MAPTS) was incorporated into chitosan or chitosan-BC matrix, regardless of the contained amount. SEM images showed also that, as the amount of K-MAPTES increases in the three analyzed series, the pores of cryogels diminish, creating smoother interstitial spaces. It can also be noted that the presence of BC in the structure of the samples did not bring any significant modifications to the cryostructures morphology.

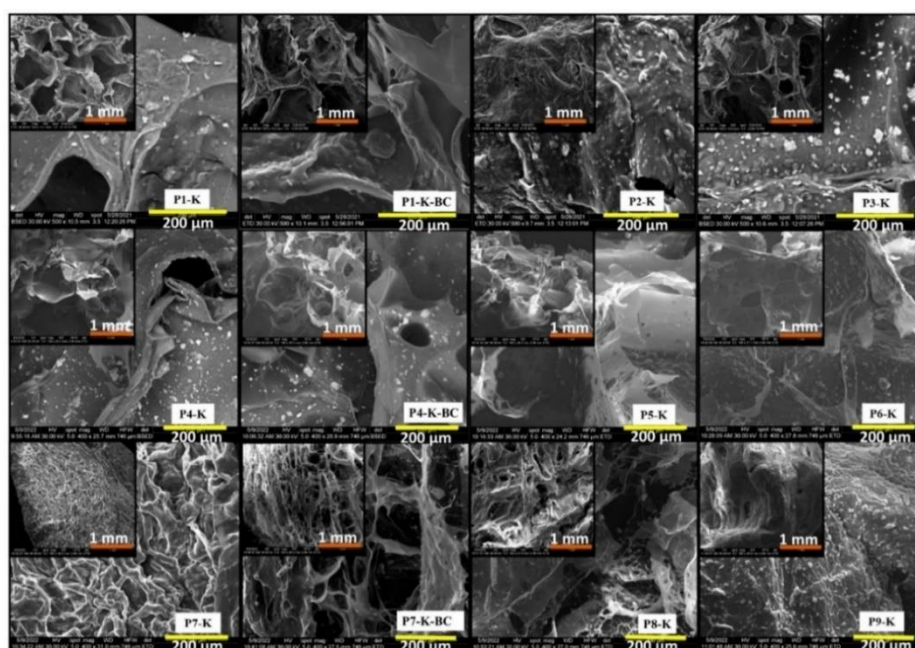


Figure 5.5. SEM images for lyophilized hybrid cryogels at 1 mm (medallion) and 200 μm scale, series P1-K-BC÷P3-K (up), P4-K-BC÷P6-K (middle) and P7-K-BC÷P9-K (bottom).

Nitrogen Intrusion Porosimetry, Brunauer–Emmett–Teller (BET)

N_2 adsorption–desorption isotherms, based on Brunauer, Emmett, and Teller’s (BET) theory principles allowed the determination of BET specific surface area, pore volume (V_p), a specific surface area of pores (S_{BET}), pore surface area (A_p), and average pore diameter (D_p), of all the cryostructures series and reference counterparts (K-MAPTES, K) (**Table 5.4.**).

The cryostructures showed similarities of textural parameters with the K and K-MAPTES references. The specific surface areas and pore volumes of cryostructures with higher K-MAPTES content (P3-K, P6-K and P9-K) are significantly higher compared to those containing lower K-MAPTES, regardless of the type of chitosan used, which means that all textural parameters are closely related to the amount of K incorporated. It can be noted, that in the case

of BC-based cryostructures, BET parameters are improved, which may be due to their fibrillated texture.

Table 5.4. BET-specific parameters for the three cryostructures series compared to K and K-MAPTES.

Sample	Surface Area BET (m ² g ⁻¹)	Pore Surface Area (BJH) (m ² g ⁻¹)	Pore Diameter for Desorption (BJH) (nm)	Pore Volume (BJH) (Measured la P/P0 = 0.99) (cm ³ g ⁻¹)
K-MAPTES	7,373	9,216	28,750	0,034
K	9,703	10,010	3,169	0,024
P1-K	1,812	3,253	3,627	0,005
P1-K-BC	2,310	4,279	4,152	0,006
P2-K	3,705	6,177	4,152	0,010
P3-K	3,067	11,400	4,152	0,013
P4-K	1,318	2,273	4,752	0,004
P4-K-BC	2,213	3,068	4,543	0,005
P5-K	2,851	3,212	4,543	0,007
P6-K	3,980	5,053	4,543	0,010
P7-K	1,720	2,310	3,315	0,005
P7-K-BC	1,967	5,068	3,627	0,008
P8-K	6,484	9,480	3,969	0,018
P9-K	8,322	11,300	4,152	0,023

The N₂ adsorption and desorption isotherms of K, K-MAPTES and the three series of cryostructures that showed H4-type hysteresis curves are characteristic of mesoporous structures according to the IUPAC classification [246]. This type of isotherm is recorded for mesoporous adsorbent with cylindrical pores that cause hysteresis formation upon gas desorption [249]. However, the hybrid cryostructures showed 4 representative peaks, which suggested the presence of mesopores with diameters ranging from 3.169 to 4.152 nm, while for K and K-MAPTES only 3 representative peaks were observed, most of the mesopores having a diameter of 28.5 nm.

Determination of the Swelling Degrees (SDs)

The variation in time of SDs for the cryostructures samples, shown in **Table 5.5**. From this study, it was found that the water stability of cryostructures is low because they are not chemically cross-linked [250]. The highest stability in water was obtained for the CC-based samples (up to 2 h), followed by the CSH series (up to 1 h) and finally the CCH-based which started to fragment after only 45 min. However, the GGs reported in the present study were comparable to those presented by Neblea et al. [250], with the difference that the high GG values in the present case were obtained in a very short time, 1-2 h of swelling, which may be due to the fact that these cryostructures were not chemically cross-linked.

Table 5.5. Swelling degrees in time for all the cryostructures in distilled water.

Time (min)	SD (g H ₂ O/ g Cryostructure)											
	P1-K-BC	P1-K	P2-K	P3-K	P4-K-BC	P4-K	P5-K	P6-K	P7-K-BC	P7-K	P8-K	P9-K
5	7,0	5,8	2,2	3,5	109,3	76,4	35,1	10,2	0,79	1,6	1,1	2,2
15	10,1	7,6	3,0	4,2	159,9	136,4	44,5	17,2	2,11	3,2	3,0	6,3
30	16,6	13,2	4,5	8,0	193,7	148,7	52,8	19,42	3,4	7,8	5,8	12,8
45	19,8	16,5	6,6	14,1	195,0	168,8	60,6	19,62	5,0	16,7	9,5	26,8
60	23,1	20,1	9,0	19,6	-	-	-	-	6,0	30,8	14,8	32,7
120	31,9	36,6	19,5	35,2	-	-	-	-	-	-	-	-

It is important to note that by increasing the amount of K-MAPTS incorporated into the polymer matrix, a favourable effect on the degree of swelling was observed only for the CC and CCH series of cryostructures. In these cases, the samples with higher K-MAPTS content, namely P3-K and P6-K, appear to show moderate water adsorption over time compared to the samples with lower K-MAPTS content, namely P1-K and P4-K, respectively. Also, for these series, BC leads to even higher water adsorption, which ultimately accelerates the fragmentation process of the cryostructures.

Following these results, it can be seen that the addition of K-MAPTS can lead to an increase in the stability of cryostructures at pH values of 5.5 in distilled water, considering the few studies reporting measurements of chitosan physical gels below pH 6-7 (due to their pH sensitivity).

Evaluation of PG Retention by Batch Adsorption Measurements

For all series of cryostructures, adsorption capacity was studied using PG as the target antibiotic. Its high solubility in water made the study laborious. However, due to PG's tendency to decompose rapidly in aqueous solutions, forming penicilic acid in as little as 24 hours [253], the decrease in PG from the supernatant solution was evaluated against the adsorption recorded for the 0.02 mol/L PG solution, freshly measured at each time interval. The retention capacities of PG on cryostructures can be seen in **Figure 5.11** and **Table 5.6** respectively. The addition of PG increases the pH of the solution from 5.5 (distilled water) to 6.5, which prevents fragmentation of the cryostructures. This explanation is the reason why the samples were much more stable compared to GG. For the CC and CCH series (**Figure 5.11 a, b**), the cryostructures containing BC, show the highest adsorption capacities of 21.1 and 16.1 mmol/g, respectively, after 24 h.

Valorificarea chitosanului din surse marine pentru obținerea unor noi agenți de tratare a apelor

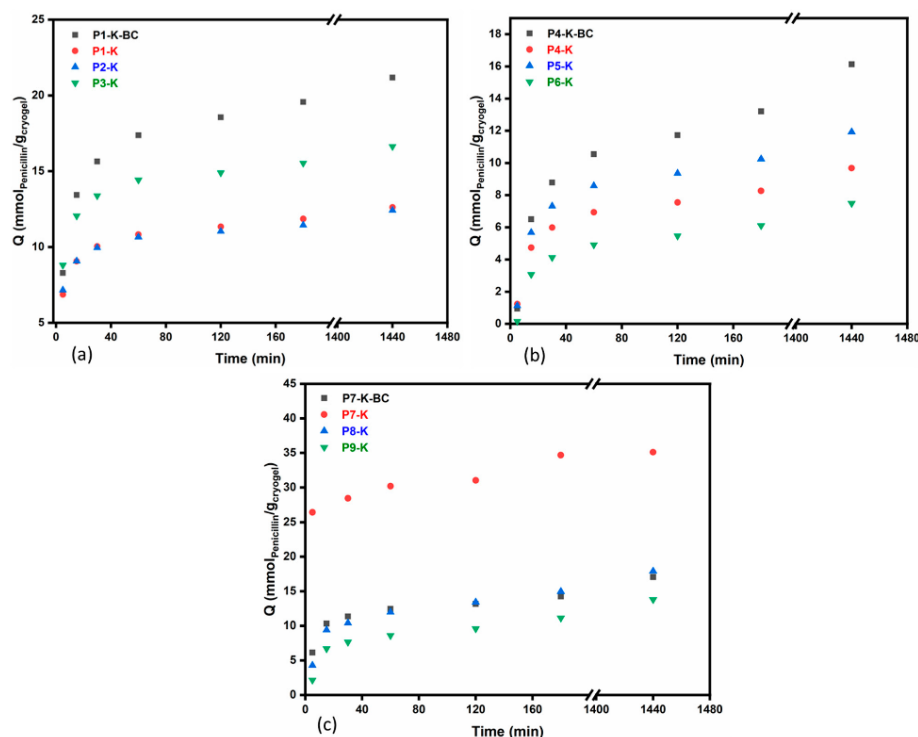


Figure 5.11. Profiles of PG retention in time for the cryogel series based on CC (a), CCH (b), and CSH (c), performed in distilled water at room temperature.

Table 5.6. Adsorption capacities of cryostructures for PG [mmol/g], starting at 0.02 mol/L solution

Time (min)	Q (mmolPG/g cryostructure)											
	P1-K-BC	P1-K	P2-K	P3-K	P4-K-BC	P4-K	P5-K	P6-K	P7-K-BC	P7-K	P8-K	P9-K
5	8,3	6,8	7,1	8,8	0,9	1,2	1,1	0,2	6,1	26,4	4,3	2,2
15	13,4	9,1	9,0	12,0	6,5	4,7	5,7	3,0	10,3	37,5	9,4	6,7
30	15,6	10,0	9,9	13,3	8,8	5,9	7,3	4,1	11,4	28,4	10,4	7,6
60	17,3	10,8	10,6	14,4	10,5	6,9	8,5	4,9	12,4	30,1	12,0	8,6
120	18,5	11,3	11,0	14,9	11,7	7,5	9,3	5,4	13,1	31,0	13,4	9,6
180	19,5	11,8	11,4	15,5	13,2	8,2	10,2	6,1	14,2	34,7	14,9	11,1
1440	21,1	12,6	12,4	16,6	16,1	9,6	11,9	7,5	17,0	35,1	17,9	13,8

In the case of the CSH series cryostructures, sample P7-K recorded the highest value of adsorption capacity (35.1 mmol/g), while the lowest value was for sample P9-K (13.8 mmol/g). However, the three series of cryostructures showed massive improvements in adsorption capacity for PG compared to other similar studies. Therefore, the results show that CSH and K-MAPTS based cryostructures achieve up to 5-fold higher adsorption capacity of PG in 1 h compared to other adsorbents in the literature.

In **Table 5.7.** the parameters obtained by fitting the adsorption data into a pseudo-second-order kinetic model proposed by Ho and McKay [257] are also consistent with porosity

Valorificarea chitosanului din surse marine pentru obținerea unor noi agenți de tratare a apelor

measurements. According to the literature, plots based on the graphical representation of $t/q(t)$ as a function of t show a linear relationship [258] (data shown in **Figure 5.12. (a), (b), (c)**). With the exception of the P4-K-BC sample, the data are consistent with the selected kinetic model, given that all R^2 values have a value close to 1, which means that the model correctly describes the investigated dependence [258].

Table 5.7. Parameters fitting for PG adsorption according to a pseudo-second-order kinetic model.

Sample	k_2 (g mg ⁻¹ min ⁻¹)	q_e (mg/g)*	R^2
P1-K-BC	$5,37 \cdot 10^{-6}$	7537	0,9999
P1-K	$1,23 \cdot 10^{-5}$	4491	0,9999
P2-K	$1,17 \cdot 10^{-5}$	4423	0,9999
P3-K	$9,31 \cdot 10^{-6}$	5918	0,9999
P4-K-BC	$2,04 \cdot 10^{-6}$	5742	0,9985
P4-K	$5,34 \cdot 10^{-6}$	3445	0,9998
P5-K	$3,99 \cdot 10^{-6}$	4247	0,9996
P6-K	$2,66 \cdot 10^{-5}$	2669	0,9995
P7-K-BC	$3,83 \cdot 10^{-6}$	6077	0,9995
P7-K	$5,77 \cdot 10^{-6}$	13362	0,9999
P8-K	$2,93 \cdot 10^{-6}$	6378	0,9996
P9-K	$2,98 \cdot 10^{-6}$	4915	0,9993

* For this evaluation, the adsorption capacity at 24 hours was used as the equilibrium adsorption capacity.

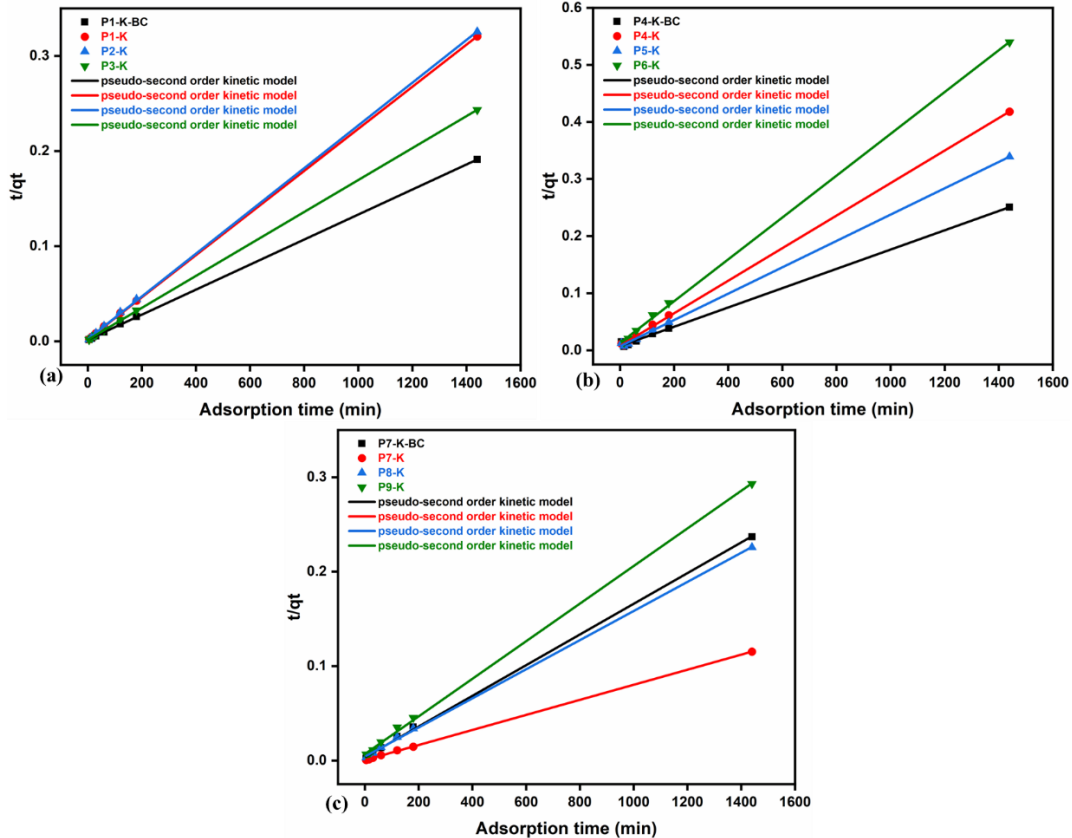


Figure 5.12. Pseudo-second order kinetic model for the series of cryostructures based on CC (a), CCH (b) and CSH (c).

Valorificarea chitosanului din surse marine pentru obținerea unor noi agenți de tratare a apelor

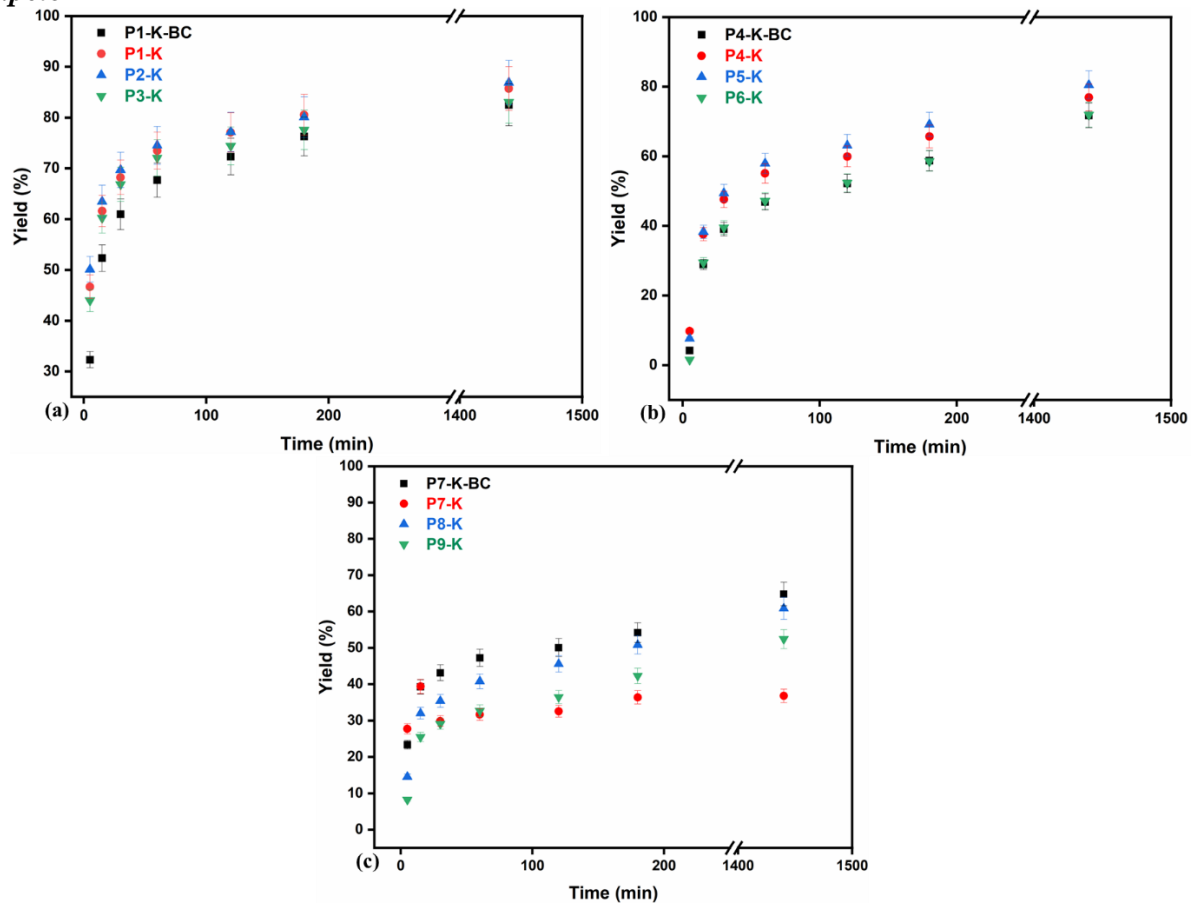


Figure 5.13. Retention efficiency of hybrid cryostructures using 5% (standard error)

In **Figure 5.13**, it may be observed the retention yield of all the cryostructures studied. For the series of CC-based cryostructures the highest retention yield was recorded for sample P2-K (86.88 %), the other samples also having quite high values. Comparing these results with the series of CCH-based cryostructures where the values were slightly lower, the highest value being for sample P5-K (80.44%), it can be considered that the first two series of cryostructures had similar retention behaviour. However, in the case of the CSH-based cryostructures, they had a rather high retention efficiency in the first 5 minutes, and then retained up to 64.80% in the case of sample P7-K-BC. These results confirm the retention capacity of the materials for PG antibiotic of about 70%- 87%.

6. RETENTION OF CIPROFLOXACIN AND CARBAMAZEPINE FROM AQUEOUS SOLUTIONS USING CHITOSAN-BASED CRYOSTRUCTURED COMPOSITES

The third part of this PhD thesis contains the synthesis and characterization of composite cryostructures for the retention of Ciprofloxacin and Carbamazepine.

Two series of cryostructures based on commercial chitosan (C1-K,C1-OS), and chitosan prepared from shrimps shells waste enriched with calcium carbonate (C2-K, C2-OS) modified kaolin and silicate prepared by sol-gel method according to **Figure 6.1.** were prepared for CIP and CBZ retention.

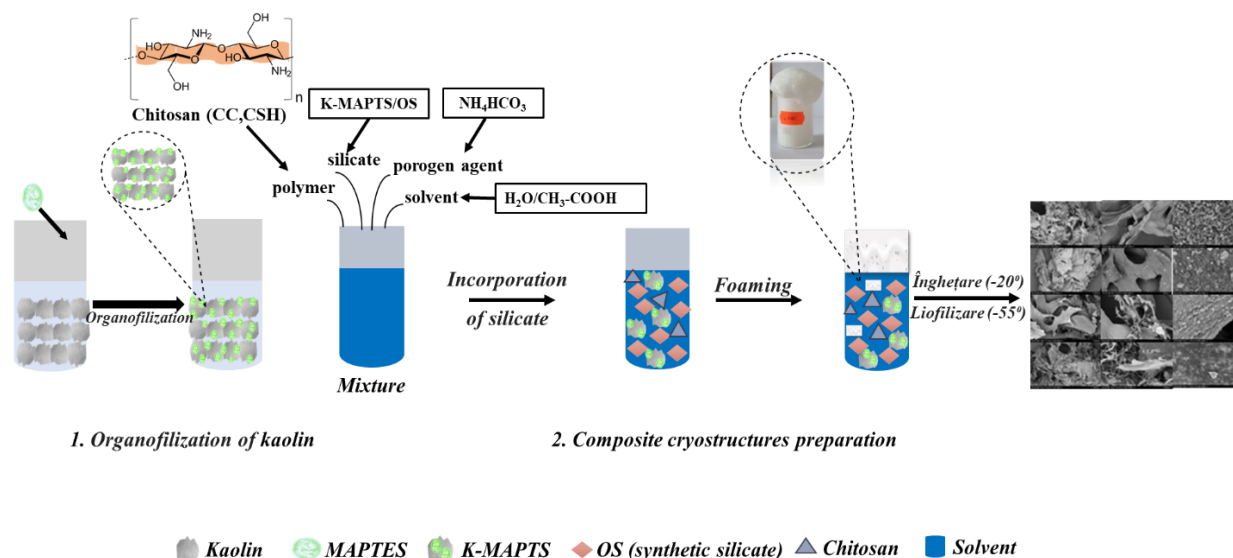


Figure 6.1. Synthesis of composite cryostructures based on natural polymers and silicates.

FTIR Spectroscopy

The FTIR spectra for composite materials prepared using two types of chitosan CC and CSH and two different silicates (K and OS) are shown in **Figure 6.2.** The spectra of the two composite cryostructures containing K-MAPTES (**Figure 6.2.**) are similar as the only difference is the type of chitosan. The same structural similarity was also observed for the series of cryostructures containing OS (**Figure 6.2.**). In **Figure 6.2.** the chitosan-specific bands were observed in the same spectral ranges as described above. While for the polymeric structure of OS (Si-O-Si) it is visible at 1082 cm^{-1} and 795 cm^{-1} . Thus, the FTIR spectra confirm that silicates have been successfully incorporated into the chitosan matrix [264-266].

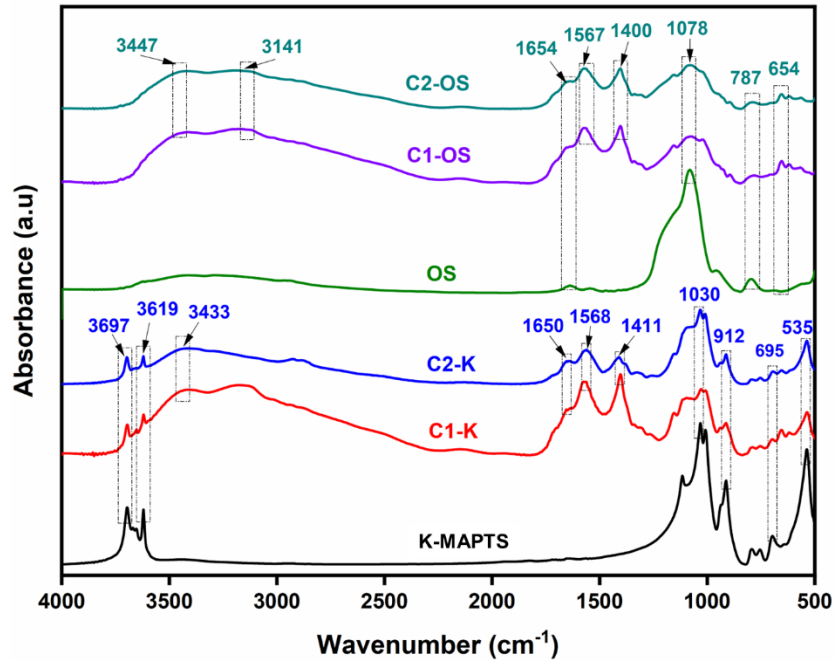


Figure 6.2. FTIR spectra for composite cryostructures (a) C1-K, C2-K series; (b) C1-OS, C2-OS series, compared with K-MAPTS and OS spectra, respectively.

Scanning Electron Microscopy (SEM)

In order to confirm the incorporation of silicates into the chitosan polymer matrix and to be able to analyse the morphology of the prepared cryostructures, the SEM technique was used (**Figure 6.2.**).

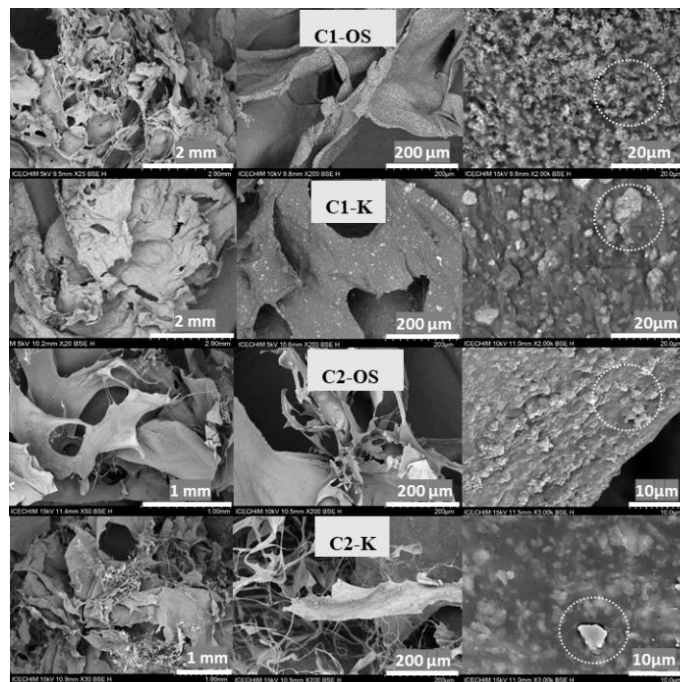


Figure 6.3. SEM images for composite cryostructures (a) series based on CC (C1-K, C2-K); (b) series based on CSH (C1-OS, C2-OS).

Valorificarea chitosanului din surse marine pentru obținerea unor noi agenți de tratare a apelor

Composites cryostructures show small morphological differences depending on the type of chitosan, but also due to the silicate used. Cryostructures prepared using CC are more compact, with smaller pores and relatively smooth surfaces, while cryostructures with CSH exhibit a more fibrillated morphology as exposed at 200 μm. At 10 and 20 μm, the presence of K-MAPTS, with particle sizes of 1-2 μm, and that of silicate OS, with particle diameters of about 300-400 nm, can be observed.

Swelling Degrees Study (GG)

Swelling degrees (SG) for all composite cryostructures were tested at different pH values (4, 7 and 9) to see their behaviour, since in the previous study [244] it was observed that at pH 5.5 cryostructures start to disintegrate after only 1 or 2 hours. Each sample (0.01 g) was placed in contact with 10 ml of solution (pH 4, 7 or 9) in a 50 ml Falcon tube at 220 rpm. GG of these macroporous composites confirms that if the pH is increased, each sample is able to resist for a longer time, but with the consequence of not being able to adsorb a larger amount of water. Furthermore, although the test time was 4 hours, samples tested at pH 9 show lower GG values. CSH-based samples showed the best GG values, especially C2-OS, for which a maximum water adsorption capacity was recorded. As in the previous studies, the behaviour of the samples is due to the physical cross-linking of the cryostructures.

Table 6.2. Swelling degrees for cryostructures at different pH values (4.7 and 9)

Time (min)	SD (g H ₂ O/ g Cryostructure) pH=4				SD (g H ₂ O/ g Cryostructure) pH=7				SD (g H ₂ O/ g Cryostructure) pH=9			
	C1-K	C2-K	C1-OS	C2-OS	C1-K	C2-K	C1-OS	C2-OS	C1-K	C2-K	C1-OS	C2-OS
5	6,51	6,93	5,60	5,18	4,34	2,71	5,37	3,95	5,09	5,39	7,17	5,60
15	6,25	12,86	6,64	12,66	4,12	3,55	5,10	5,79	5,51	6,01	7,50	7,67
30	6,32	18,93	8,35	13,87	4,11	4,35	4,62	6,14	6,40	6,25	7,62	8,01
60	6,39	19,81	9,45	14,61	4,32	4,75	4,75	6,48	6,97	6,33	8,10	8,48
120	7,24	20,47	11,70	14,72	4,95	5,05	4,63	6,56	7,00	6,73	8,15	8,56
180	7,38	21,35	12,55	15,18	5,46	5,35	4,79	6,93	7,30	7,15	8,36	9,36
240	-	-	-	-	-	-	-	-	7,73	7,68	8,40	10,24

All samples were tested between different deformation ranges, as can be seen in Figure 6.4. The samples become thinner and compress (densification process) due to the force applied (50 N cell) on their macroporous structure, but do not completely destroy themselves after analysis. From the data collected, it can be concluded that C1-K did not require a large force to break the structure, unlike the C2-OS and C2-K cryostructures. The maximum deformation for C2-K and C2-OS samples was higher (between 84-122%) compared to C1-K, for which less than 5.5% deformation was recorded at the time of fracture.

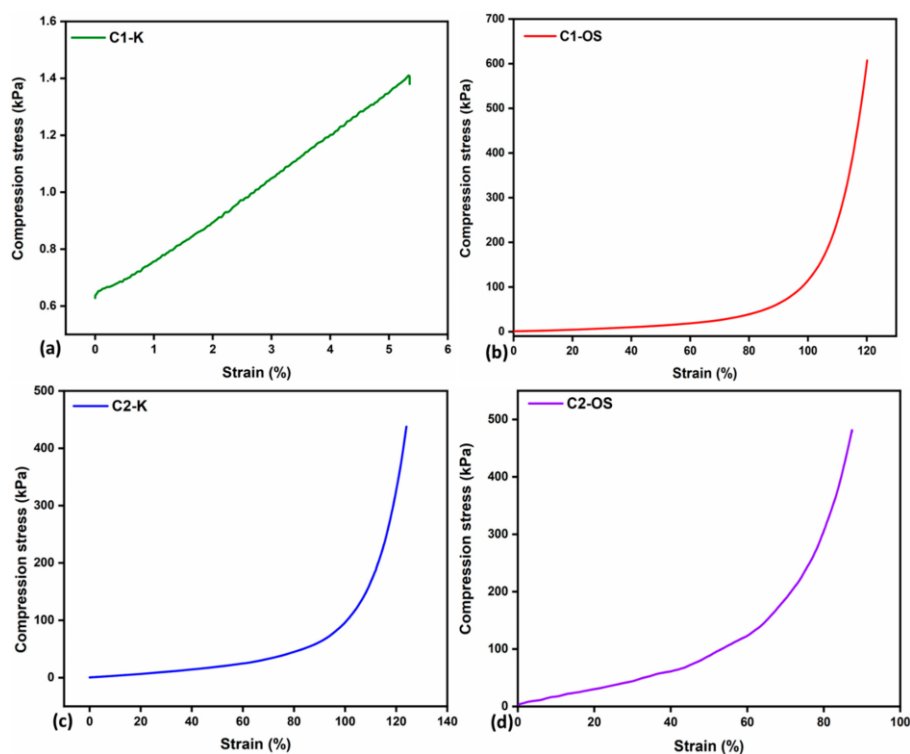
Valorificarea chitosanului din surse marine pentru obținerea unor noi agenți de tratare a apelor

Figure 6.4. Compression results of cryostructures based on C1 (C1-K (a), C1-OS (b)) and based on C2 (C2-K (c), C2-OS (d)).

The results suggest that the chitosan-containing sample from the shrimp shells waste is a contributing factor to improved mechanical properties, along with the fact that OS leads to greater homogeneity and therefore improved mechanical stability, regardless of the type of chitosan. The Young's modulus shows the following values, calculated from the slope of the initial linear part of the curve (elastic region): C1-K - 13 kPa; C1-OS - 40 kPa; C2-K - 33 kPa; C2-OS - 167 kPa. The results indicate a deformation range of 85-120% for the chitosan-based samples compared to other studies (where the deformation was 85% maximum) [268].

Evaluation of the retention capacity of the two series of cryostructures for CBZ and CIP

Since commercial chitosan (CC) based systems were not shown to be very stable, the kinetic process was only evaluated for C2-K and C2-OS samples. Several experiments were performed to study the influence of time on the retention capacity of composite cryostructures for the two drugs CIP and CBZ at $\text{pH } 6.0 \pm 0.5$. As can be seen in **Figure 6.5.** and **Table 6.3.** the maximum adsorption capacity after 24 h of C2-K for CBZ and CIP, was 12.95 mg/g and 5.16 mg/g, respectively, compared to C2-OS, which recorded 9.77 mg/g and 3.69 mg/g of the same drugs. As also summarized in **Table 6.3,** maximum yields were recorded after 24 h for C2-K, up to 86.38% CBZ and 85.94% CIP, compared to C2-OS, which only managed to retain 65.11% CBZ and 61.63% CIP.

Valorificarea chitosanului din surse marine pentru obținerea unor noi agenți de tratare a apelor

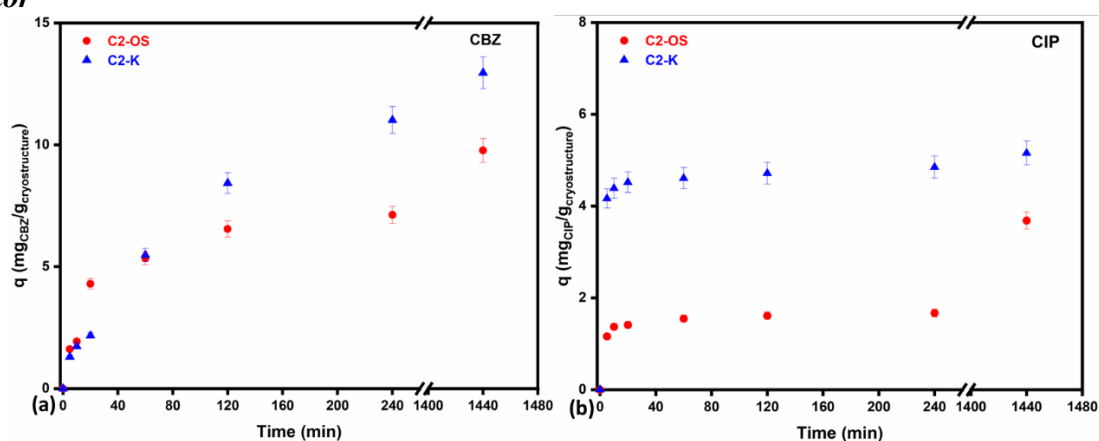


Figure 6.5. Adsorption capacity for the series of cryostructures on two drugs CBZ (a) and CIP (b) applying a standard error of 5%.

Table 6.3. Adsorption capacity for the series of cryostructures on two drugs CBZ (a) and CIP (b), applying a standard error of 5%.

Time (min)	CBZ				CIP			
	q (mg/g _{cryostructure})		Y (%)		q (mg/g _{cryostructure})		Y (%)	
	C2-K	C2-OS	C2-K	C2-OS	C2-K	C2-OS	C2-K	C2-OS
5	1,30	1,62	8,66	10,79	4,14	1,16	69,40	19,36
15	1,73	1,94	11,56	12,93	4,39	1,31	73,13	22,85
30	2,18	4,30	14,52	28,67	4,52	1,41	75,29	23,55
60	5,48	5,35	36,51	35,65	4,61	1,55	76,82	25,82
120	8,42	6,55	56,17	43,66	4,71	1,61	78,58	26,89
240	11,01	7,12	73,43	47,49	4,85	1,67	80,80	27,84
1440	12,95	9,77	86,36	65,11	5,16	3,69	85,94	61,43

The adsorption behaviour for CBZ and CIP was described by kinetic models: pseudo 1st and 2nd order kinetic models, intraparticle diffusion and Elovich. The plots can be seen in Figures 6.7., 6.8., 6.9., 6.10., for CBZ and for CIP, and the parameters in Table 6.4.

The intraparticle diffusion model can be applied to porous materials, such as those obtained in this study, where equilibrium is reached in the pores of the material by diffusion mechanisms [269]. However, it appears that several processes influence the adsorption equilibrium, such as chemisorption. Which is why the Elovich kinetic model was also correlated with the obtained data. This model is suitable for systems with heterogeneous adsorbent surfaces, especially to prove that chemical adsorption (chemisorption) has occurred [270]. In this case, it can be seen that the Elovich model is more suitable for CBZ adsorption, but still does not describe the adsorption behaviour very well, especially for CIP. Therefore, the most suitable model for this mechanism seems to be the pseudo- second order kinetic model, which argues that the main limiting factor of the adsorption process is chemisorption and thus the adsorption rate is influenced by the adsorption capacity and not by the initial concentration

Valorificarea chitosanului din surse marine pentru obținerea unor noi agenți de tratare a apelor

[271]. The results indicate that drugs were adsorbed on the surface and in the pores of the composite materials. Therefore, for CBZ adsorption, the accuracy of the kinetic models was as follows: (i) pseudo-second order kinetic model > intraparticle diffusion model > Elovich > pseudo-order I kinetic model for the C2-K sample and (ii) pseudo-second order kinetic model > Elovich > intraparticle diffusion model > pseudo-first order kinetic model for the C2-OS system. While for CIP adsorption, the appropriate sequence was (i) pseudo-second order kinetic model > Elovich > intraparticle diffusion model > pseudo-first order kinetic model for C2-K system and (ii) pseudo-second order kinetic model > intraparticle diffusion model > Elovich > pseudo-first order kinetic model for C2-OS system.

According to the literature it has also been shown that the best regressions were obtained using the pseudo-second order kinetic model for CIP [272] and CBZ [273,274].

Table 6.4. Parameters of kinetic models for CBZ and CIP

Kinetic model	Kinetics parameters	CBZ		CIP	
		C2-K	C2-OS	C2-K	C2-OS
pseudo-first ordin	$K(g\ mg^{-1}\ min^{-1})$	$8,50 \times 10^{-3}$	$18,00 \times 10^{-3}$	$430,00 \times 10^{-3}$	$68,00 \times 10^{-3}$
	$qe\ (mg/g)$	12,95	9,76	5,15	3,68
	R^2	0,992	0,927	0,980	0,490
pseudo-second ordin	$K_2(g\ mg^{-1}\ min^{-1})$	$93,0 \times 10^{-3}$	$1,98 \times 10^{-3}$	17,17	36,35
	$qe\ (mg/g)$	12,95	9,76	5,15	3,68
	R^2	0,995	0,998	0,999	0,984
difusion intraparticulă	$K_p(g\ mg^{-1}\ min^{-1/2})$	0,33	0,21	0,02	0,07
	$C(mg/g)$	2,16	2,73	4,34	0,96
	R^2	0,752	0,789	0,833	0,959
Elovich	$\alpha\ (mg\ g^{-1}\ min^{-1})$	0,42	0,68	6,16	2,72
	$\beta\ (g/mg)$	-3,42	-0,74	3,96	0,28
	R^2	0,949	0,979	0,980	0,703

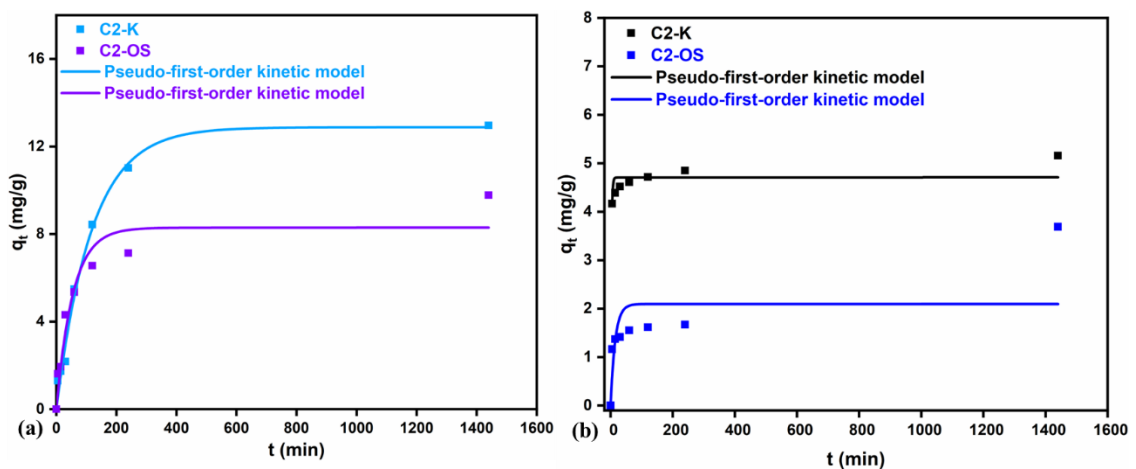


Figure 6.7. Non-linear regression for the pseudo-first order kinetic model for **CBZ (a)** and **CIP (b)**.

Valorificarea chitosanului din surse marine pentru obținerea unor noi agenți de tratare a apelor

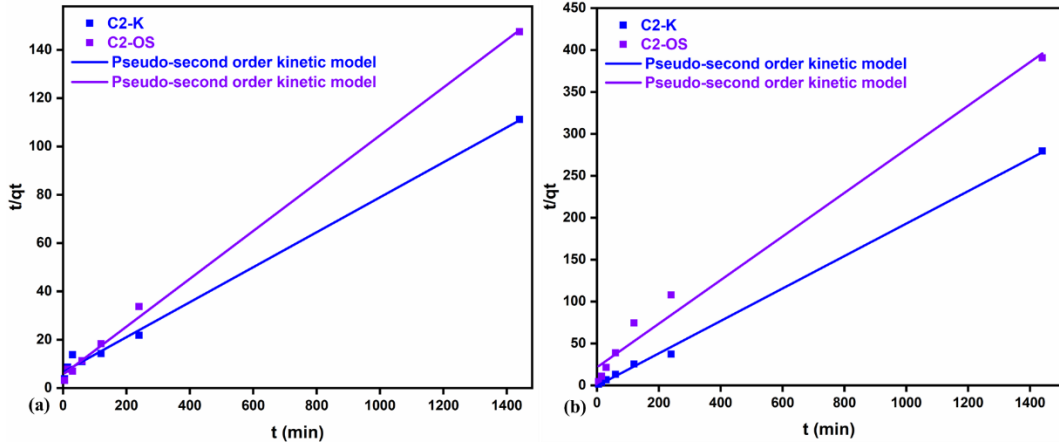


Figure 6.8. Linear regression for the pseudo-second order model for **CBZ** (a) and **CIP** (b).

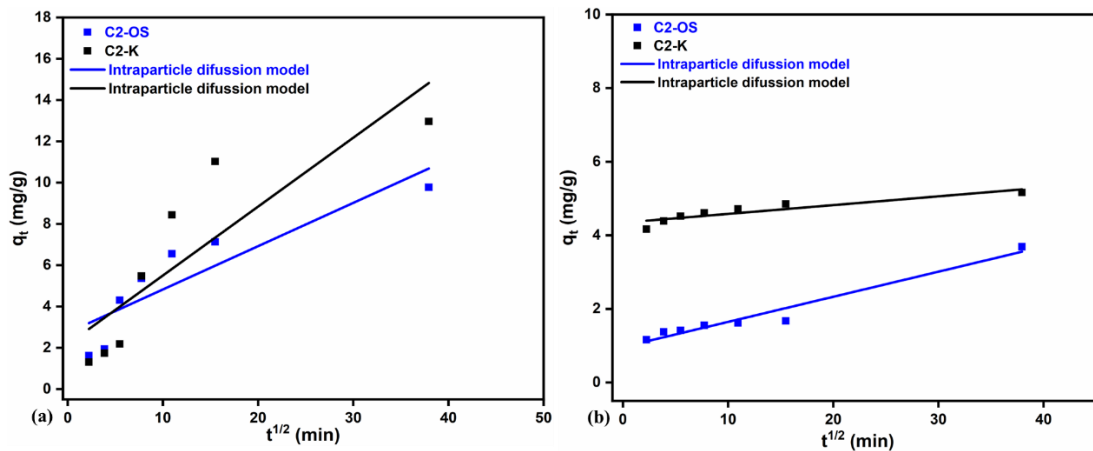


Figure 6.9. Linear regression for intraparticle diffusion model of for **CBZ** (a) and **CIP** (b)

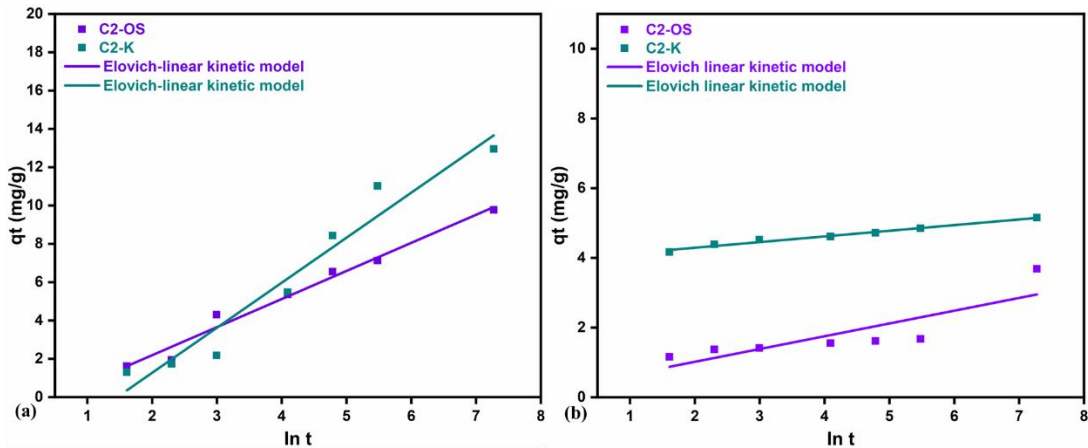


Figure 6.10. Linear regression for the Elovich kinetic model for **CBZ** (a) and **CIP** (a)

Its worth mentioning that by changing the reinforcement agent-K-MAPTS to a synthetic silicate-OS some improvements in the mechanical stability of physically cross-linked chitosan-based cryostructures were obtained, but with an obvious loss of drug retention capacity. However, the results in both cases are promising compared to other studies, as the obtained composite materials are effective in removing CBZ or CIP from aqueous solutions (15 mg/L CBZ and 6 mg/L CIP) compared to other studies [275-276].

GENERAL CONCLUSIONS

The PhD thesis "*Valorization of chitosan from marine sources for obtaining water treatment agents*" aimed, based on the study of literature, to synthesize and characterize new types of high performance materials, in the form of cryostructures based on natural polymers and silicates, for the retention of drugs from polluted waters. Each type of material was characterized structurally, morphologically and thermally, and adsorption and kinetics experiments demonstrated their applicability.

The results obtained converge towards the following general conclusions:

In *chapter 4*, new materials, namely molecularly imprinted pseudo-cryogels for drug retention using natural polymers, were obtained. Commercial chitosan and biocellulose were used as precursors and the antibiotic PG was selected as targeted molecule. Characterization techniques confirmed the imprinting of PG in the structure of the MIP pseudo-cryogels. MIP samples retained up to 2-fold more PG than those reported in other studies. The best result was obtained for the biocellulose and chitosan-based MIP pseudo-cryogel prepared in the laboratory, with an IF=1.24 after 5 minutes of contact. The adsorption process was confirmed by pseudo-second order kinetic model.

In *chapter 5*, hybrid cryostructures were prepared for antibiotic retention using natural polymers and clays. Three types of chitosan (CC, CCH, CSH) were used together with BC and K-MAPTS to improve the material properties. Characterization techniques confirmed the retention capacity of PG-approved. CSH and K-MAPTS based samples had a retention capacity of 10.742 mg PG/g cryostructure after only 60 minutes. The kinetics revealed a mechanism of PG adsorption using a pseudo second order kinetic model for all cryostructures analyzed. The stability of the samples is influenced by the pH of the solutions, with the samples lasting up to 24 hours at a pH close to 6.5. The results confirm that chitosan and modified kaolin-based materials are effective in PG retention, with significant potential for their application in wastewater treatment.

In *chapter 6* chitosan-based composite cryostructures for CBZ and CIP retention were developed. The use of a synthetic silicate instead of K-MAPTS improved the mechanical strength and water resistance of the cryostructures. Characterization techniques confirmed the incorporation of silicates into cryostructures. Compression tests confirmed the improved behaviour. The C2-K sample adsorbed large amounts of CBZ and CIP with yields of 86.38% and, 85.94%. The pseudo-order II kinetic model was the best fit, indicating a major contribution of chemisorption on the overall adsorption process for both CBZ and CIP.

REFERENCES

207. Sadeghi, M.; Moradian, M.; Tayebi, H.-A.; Mirabi, *Chemosphere* **2023**, *311*, 136887..
245. Ho, Y.S.; McKay, G., *Chemical Engineering Journal* **1998**, *70*, 115–124.
246. ALothman, Z.A., *Materials* **2012**, *5*, 2874–2902.
249. Thommes, M.; Kaneko, K.; Neimark, A.V.; Olivier, J.P.; Rodriguez-Reinoso, F.; Rouquerol, J.; Sing, K.S.W., *Pure and Applied Chemistry* **2015**, *87*, 1051–1069.
250. Neblea, I.E.; Chiriac, A.-L.; Zaharia, A.; Sarbu, A.; Teodorescu, M.; Miron, A.; Paruch, L.; Paruch, A.M.; Olaru, A.G.; Iordache, T.-V, *Polymers* **2023**, *15*, 1091.
253. Wang, F.-X.; Prokes, I.; Song, L.; Shi, H.; Sadler, P.J. *J Biol Inorg Chem* **2022**, *27*, 695–704.
258. Plazinski, W.; Dziuba, J.; Rudzinski, W., *Adsorption* **2013**, *19*, 1055–1064.
264. Dinu, M.V.; Humelnicu, I.; Ghiorghita, C.A.; Humelnicu, D. *Gels* **2022**, *8*, 221.
265. Biswas, S.; Rashid, T.U.; Mallik, A.K.; Islam, M.M.; Khan, M.N.; Haque, P.; Khan, M.; Rahman, M.M., *International Journal of Polymer Science* **2017**, *2017*, e6472131.
266. Dey, S.C.; Al-Amin, M.; Rashid, T.U.; Ashaduzzaman, M.; Md Shamsuddin, S., *ILCPA* **2016**, *68*, 1–9.
269. Wang, J.; Guo, X., *Chemosphere* **2022**, *309*, 136732.
270. Nezhadali, A.; Koushali, S.E.; Divsar, F., *Journal of Environmental Chemical Engineering* **2021**, *9*, 105648.
271. Agbovi, H.K.; Wilson, L.D. Ed.; Elsevier, 2021; pp. 1–51 ISBN 978-0-12-820541-9.
272. Zhang, C.-L.; Qiao, G.-L.; Zhao, F.; Wang, Y. *Journal of Molecular Liquids* **2011**, *163*, 53–56.
273. Adeyanju, C.A.; Ogunniyi, S.; Selvasembian, R.; Oniye, M.M.; Ajala, O.J.; Adeniyi, A.G.; Igwegbe, C.A.; Ighalo, J.O., *ChemBioEng Reviews* **2022**, *9*, 231–247.
274. Jemutai-Kimosop, S.; Orata, F.; Shikuku, V.O.; Okello, V.A.; Getenga, Z.M. *Environmental Research* **2020**, *180*, 108898.
275. Al-Ghoul, N.E.; Albarghouti, G.A.; Qandeel, R.G., *Environ Monit Assess* **2023**, *195*, 821.
276. Ajduković, M.; Stevanović, G.; Marinović, S.; Mojović, Z.; Banković, P.; Radulović, K.; Jović-Jovičić, N., *Water* **2023**, *15*, 2608.